Review of Research

International Online Multidisciplinary Journal

ISSN : 2249-894X Impact Factor 3.1402 (UIF) Volume -5 | Issue - 6 | March - 2016

A SIMPLE STRATEGY FOR DECORATION OF SILVER NANOPARTICLES ON MESOPOROUS TITANIA FOR CATALYTIC APPLICATION

Ramdas K. Dhokale

Department of Chemistry, Arts, Science and Commerce College,
Naldurg, Dist. Osmanabad (MS), INDIA.
Corresponding author: rkdhokale@gmail.com

ABSTRACT :

In present investigation successfully synthesized silver nanoparticles and decorated on mesoporous TiO_2 nanoparticles. Various characterization techniques used to study optical structural and morphological properties of synthesized nanoparticles such as UV-vis spectrophotometer, X-ray- diffraction (XRD), Fourier transform infrared (FTIR), Transmission electron microscope (TEM) and Energy dispersive X-ray spectroscopy (EDAX). Catalytic application were studied by conversion of 4-nitrophenol to 4-aminophenol, it confirms that the sufficient amount of silver NPs decorated on TiO_2 shows high rated of reaction. As well as reusability study confirms synthesized nanomaterials stable and reusable.

KEYWORDS : *Synthesized silver nanoparticles, Transmission electron microscope (TEM).*

1. INTRODUCTION

'Metal nanoparticle' is term normally used to elemental metal with dimensions (width, length, or thickness) within the nanoscale range (1–100 nm). Bulk metals are typically ductile, malleable, and also possess good conductors of heat and electricity. These properties are usually resulting from delocalization of the electrons within the bulk material. In contrast, such physical properties of metal nanoparticles (NPs) are not characteristic; due to absence of electrondelocalization observed in the bulk, thus giving rise to different properties to those of the bulk counterparts. These NPs have a higher surface area-to-volume ratio to that of the bulk equivalents, making them particularly promising candidates for catalytic transformations. Also, recent horizons in controlling the particle shape and size have opened the possibility to enhance catalytic activity by providing the optimum surface properties for specific organic reactions. Tuning particle diameter or size also results in more in surface of the system for better interaction with reacting molecules. The relationship between surface of particles, metal–metal bonding, the shape and atom-packing behavior ultimately estimates the effectiveness of these NPs in their chemical transformations.

These metallic particles are highly active centers, due to their very small in size and hence these are not thermodynamically stable state of matter. Their structures at this size regime are indeed highly unstable as a result of their high surface energies due to their large area.To form stable particles, it is necessary to terminate or to support the particles during the nucleation stage in synthesis and there are a number of ways by which one can produce stable particles. Particularly, the use of porous materials with desired pore sizes and also characteristics as supports for NPs is adsorbing the catalytic sites, and hence creating a divider between the interior and exterior pore structure. The support is also inhibiting particle growth to a optimum size as well as aggregation. Furthermore, by choosing the desired properties of the porous support; one can control the geometry with size and shape of the resulting metallic NPs [1].

Metal nanoparticles (NPs) have been shown the unprecedented catalytic performance which far exceeds those of conventional metal complex catalysts. Especially, transition metal NPs are known to exhibit outstanding catalytic properties for various chemical transformations. The importance of metallic nanomaterials, based on its surface morphology, structure and phases, play immense role to enhance its properties in different applications. The catalytic, opto-electrical properties of these materials depend on their morphology viz. nanowires, nanorods, nanotubes, nanoflowers, etc [2-5]. Particularly, noble metal NPs have playing attention towards research interest since the past few years. This is due to their distinctive physical and chemical properties, and remarkable prospective for extensive applications in catalytic, optical, electronic, biological fields [6-12]. However, the few problems, include susceptible towards aerial oxidation of metals [13], instability and hence there aggregate, which causes irregularity in the structure [14-15], can retards their scope in applications. A supported metal nanoparticle is one of the best strategies to overcome these drawbacks and hence enhance its properties for further applications.

The synthesis of silver nanoparticles involves three generally distinct routes. Silver nanoparticles can form in the presence of strong reducing agents, such as sodium borohydride, hydrazine, and tetrabutyl ammonium borohydride; which is one of the easiest routes [16-17]. A second method for forming silver NPs involves the use of different types of irradiation such as the UV irradiation [17], γ-irradiation [18], ultra-sound irradiation [19], for silver ions in solution in the presence of capping agents. A third route involves prolonged heating of silver ions in solution in the presence of weak reducing agents, such as sodium citrate [20], glucose [21], dimethyl formamide [22], polyols [23], with long-chain amine, aniline, surfactant, carboxylates, and starch have been also used to stabilize silver nanostructures. [24].

In the present investigation, the efforts are focusing on the catalytic potential of metal NPs supported on inorganic materials for their unique catalytic properties in organic transformations. An important aspect of the supported metal NPs as catalysts is the interaction between the NPs and the support. In fact, through adjusting adsorption properties, support can enhance both the activity and selectivity of a catalyst by dispersing the active sites or the different types of bonding in the presence of surroundings. In order to obtain high catalytic active surface area, metallic NPs are generally dispersed on support materials, such as mesoporous carbon [25], silica [26], zeolite [27], mixed metal oxides [28], are commonly used. Sometimes support often suffers from weak distribution of metallic particles, for example, carbon support on noble metals shows weak interaction due to poor distribution of metal on carbon support which decreases active sites [29].

Vile et al. investigated the gas-phase semi-hydrogenation of propyne, an industrially relevant reaction for the purification of olefin streams, using silica-supported Ag NPs [30]. Santos et al. showed the higher catalytic efficiency of Ag-NPs supported with linear polyethylene imine (LPEI) derivative as compared bare or other supported composites [31]. The electron charge transfer from O-vacancies at the metal–substrate interface to supported Au nanostructures is one of the ideal route for O_2 activation as well as oxidation reactions [32]. The similar results related to the delocalization of electrons from oxygen vacancies in the reduced TiO_2 surface reported the alteration in the adsorption and surface diffusion of small Au particles. [33]. Oakton et al. shown the decrease in the activity in alkene and alkyne reactions by a factor 2–3, which probably due to less alkyne adsorption properties or the presence of less accessible active sites of $Ag@SiO_2$ catalysts; however a remarkable selectivity for the production of alkenes was reported [34]. Mitsudome et al. used highly efficient reusable heterogeneous catalyst hydroxyapatite-supported silver nanoparticles for hydration of diverse nitriles, including hetero aromatic ones, into amides in aqueous solutions [35].

2 EXPERIMENTAL METHODOLOGY

2.1 Synthesis of silver nanoparticles

All chemicals used, in this study, were of AR grade. In the round bottom flask, the aqueous solutions of silver nitrate, sodium dodecyl sulfate (SDS), and sodium citrate were taken. The reaction mixture was stirred continuously at 50 ^{o}C for one hour. The yellow color was noted for the resulting dispersion; which indicates the formation of SDS-capped silver nanoparticles.

2.2. Synthesis of mesoporous titania nanoparticles

Mesoporous titania NPs were synthesized by a sol–gel method. In the 250 mL round bottom flask, titanium(IV) isopropoxide with glacial acetic acid were taken and stirred for 20 min at room temperature. The aqueous solution of SDS was added into it. The content was stirred at room temperature for 1 hour. The pH of the subsequent solution was adjusted to 10.00 by adding ammonia solution. The solution was stirred at 60 ^{o}C for 2 hour and then cooled to room temperature. Then, it was calcinated at 400 ^{o}C for obtaining TiO_2 NPs [36].

2.3. Synthesis and characterization of titania supported silver nanoparticles

The general procedure of *ex situ* route was used for preparing titania supported silver NPs and discussed as follows.

6 mL of colloidal silver NPs were taken in 50 mL round bottom flask, sonicated for 15 mins. and thereafter the well dispersed silver suspension was added into mesoporous titania. Then, the dispersed precursor was also stirred for 20 min. The precursor was filtered, washed and dried for one hour at 120 ^{o}C. The precipitate was calcinated at 200 ^{o}C for 3 hour.

The similar procedure was adopted for synthesis of supported silver NPs in its different compositions from 0.0–2.0 mol% with changing the required stoichiometry of silver precursor. Similar to supported nickel NPs, the various characterization techniques were used for supported silver NPs.

2.4 Catalytic activity

To determine the catalytic activity of supported silver NPs, a model reaction is necessary. This model reaction should not continue without the catalyst and also should proceed without side reactions in the presence of NPs. The reaction should be ease to handle and monitor in order to obtain complete kinetic studies. Furthermore, the reaction should be taking place under ambient conditions with ease separation of product from the catalysts. It is important that no transformation or degradation of the supported silver NPs occurs within the experimental temperature range. Such a model reaction allows the direct comparison of the catalytic activity of supported silver NPs and a wide range of different catalytic systems and hence, in the present case, the reduction of 4-nitrophenol by sodium borohydride in the presence of supported silver NPs is taking into consideration for further studies.

For the reduction reaction, 1 mL of water taken in sample bottle and 50μL of 4-nitrophenol ($5x10^{-4}$ M) were added followed by 700 μL of aqueous $NaBH_4$ (0.01M) was added. Then titania supported silver NPs, as a catalyst, was added. The time dependent absorption spectra were measured during the progress of the reaction. It is seen that the shifting of absorption peak of 4-nitrophenol to higher wavelength due to addition of $NaBH_4$ solution in the reaction mixture. Then, this red shift was observed at 400 nm because of the formation 4-nitrophenolate ion. The kinetic analysis of this catalytic reaction was monitored with function of time and hence the rate constants under different parameters were calculated. The product was identified by comparing with the spectrum of an authentic sample 4-aminophenol.

2.5 Characterization techniques

Optical properties of the coated concrete substrate were studied by UV–visible spectrophotometer (UV3600, Shimadzu, Japan) in the range of 200–800 nm. X-ray diffraction (XRD) studies were carried out by using a Bruker D8-Advance diffractometer. The diffraction patterns were recorded in the two theta range of 10–90◦ by using Cu K (1.5418 A) ´° radiation. Fourier transform infrared (FTIR) spectra of the samples were recorded using (Nicolet™ iS™ 50 FTIR Spectrometer) in the range between 400 and 4000 $cm^{-1.}$ Transmission electron microscope (TEM) images of the samples were recorded on a Tecnai F30 field emission transmission electron microscope operating at 300 kV. Energy dispersive X-ray spectroscopy (EDAX) was recorded by using FEI Quanta 200 Environmental SEM.

3 RESULT AND DISCUSSIONS

3.1 UV-visible measurements

The UV-visible absorption spectrum of silver NPs and supported silver NPs on titania host lattice is shown in Fig.1. The absorption band at 415 nm confirms that formation of silver NPs. The observed surface plasmon absorption band of silver suspensions was different than its bulk counterparts [37]. The color of the dispersion changes from faint yellow to dark yellowish due to the higher concentration of silver NPs. However, in all the samples, the plasmon peak is almost symmetrical and there are no peaks in the range of 450–700 nm due to aggregation of silver nanoparticles [38]

The stability of silver suspensions was determined by UV-visible spectrometer. The plot of absorbance versus wavelength for silver suspension with respect to months is shown in Fig. 2. Plot shows that the wavelength of silver plasmon band remains unchanged up to 3 months reveals the formation of stable silver particles. The stability of silver colloids is attributed due to capping of silver particles in its nucleation stage and hence there is no any aggregation of the particles [39]. Fig. 3 shows UV-visible absorption spectra of mesoporous titania supported silver NPs and pure titania. In all these, the absorption band of silver particles is shifted from 415 nm to 465 nm; which is due to surroundings of supportive matric around the silver particles

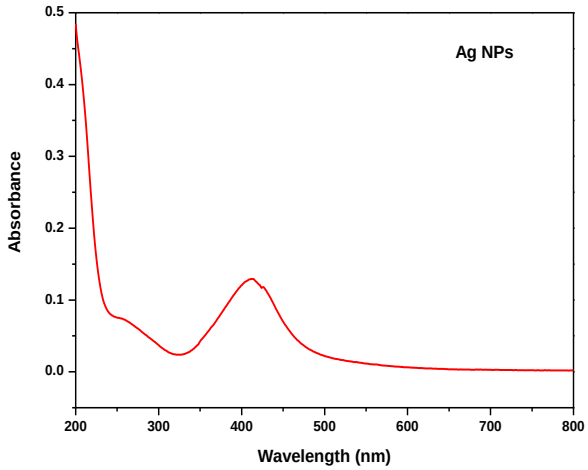

Fig. 1: UV- Visible spectrum of colloidal silver nanoparticles

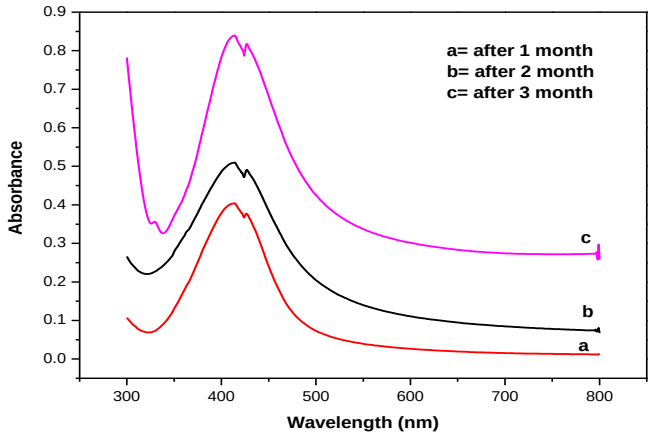

Fig.2: UV-Visible spectrum of silver nanoparticles for stability measurements

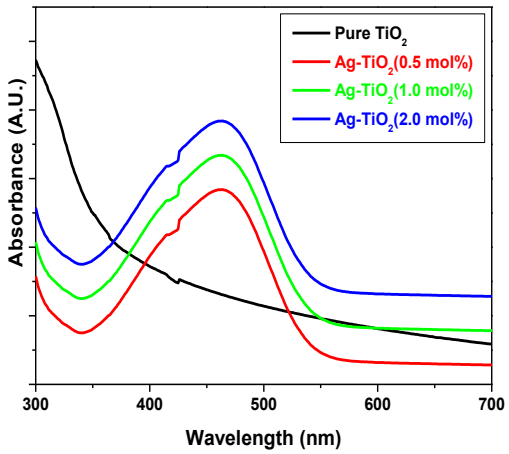

Fig. 3: UV-Visible spectrum of supported silver nanoparticles on titania host lattice

3.2 X-ray diffraction Studies

XRD measurements have also been performed to reveal the structural properties of the supported silver NPs. Fig.4 shows the XRD diffraction patterns of mesoporous titania supported silver NPs with pure titania. In patterns of the supported samples, the two diffraction peaks at 38.56, 44.21 correspond to (111), (200) reflections of elemental silver, clearly suggesting the formation of metallic silver in face centered cubic. The small shift in the peak positions reveals the attachment of silver NPs to the TiO_2 [40]. While, in all XRD patterns, other diffraction peaks shows tetragonal titania with anatase phase. The sharp peaks indicates that silver and titania present in crystalline in nature. The average crystallite sizes of TiO_2 anatase and Ag nanoparticles were calculated using the Scherrer equation:

$$D=0.94\lambda/\beta\cos\theta \ldots\ldots\ldots\ldots \quad (1)$$

Where, D is the average crystallite size, λ is the wavelength of X–ray (Cu Kα = 1.5418 Å) radiation, β is the FWHM of the diffraction peak and θ is the Bragg angle. FWHM of each diffraction line was determined from the profile measured with a scanning rate of$1/2^{o}$ (2θ) min^{-1}, which was calibrated by a standard silicon powder for instrumental broadening. For indexing the patterns, the phases were identified with the aid of the Joint Committee on Powder Diffraction Standards (JCPDS) [41]. The structural parameters of the representative supported silver nanoparticles with titania are shown in Table .1.

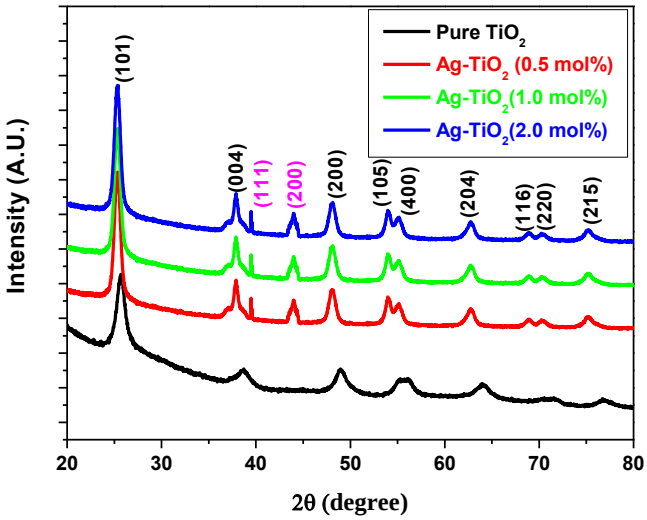

Fig. 4: XRD patterns of TiO_2 and Ag decorated TiO_2 nanoparticles.

Table 1: The structural parameter of Ag/TiO_2 and TiO_2 NPs based on XRD analysis

Samples		Std. *d* values (Å)	Obser. *d* values (Å)	(hkl)	Cell cons. a and c (Å)	Crystallite size (nm)	Crystal system
Ag/TiO_2 (2.0 mol%)	TiO_2	3.5140	3.5571	(101)	3.8004	13.34	Tetragonal
		2.3755	2.3458	(004)	9.3832		
		1.3372	1.3436	(220)			
	Ag	2.3200	2.3197	(111)	4.1016	23.50	Face–centered cubic
		2.0500	2.0508	(200)			
TiO_2		3.5140	3.5133	(101)	3.7839	8.59	Tetragonal
		2.3755	2.3648	(004)	9.4799		
		1.3372	1.3418	(220)			

3.3 Transmission electron microscope (TEM) studies

TEM images of pure titania and titania supported silver NPs are shown in the Fig. 5 (a) and (b) respectively. The particles size of titania was observed within range of 25-30 nm, while dark spot of silver NPs observed on the lighter region of titania surface. These pictures reveal that silver NPs are supported on surface of the titania. The particle size of silver NPs are 15-20 nm [42].

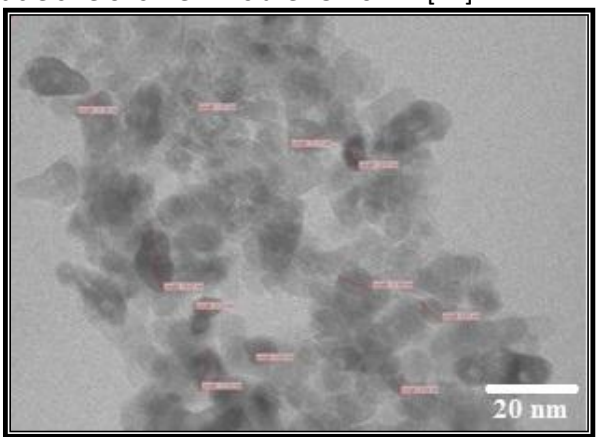

Fig. 5.(a) :TEM image of pure titania NPs

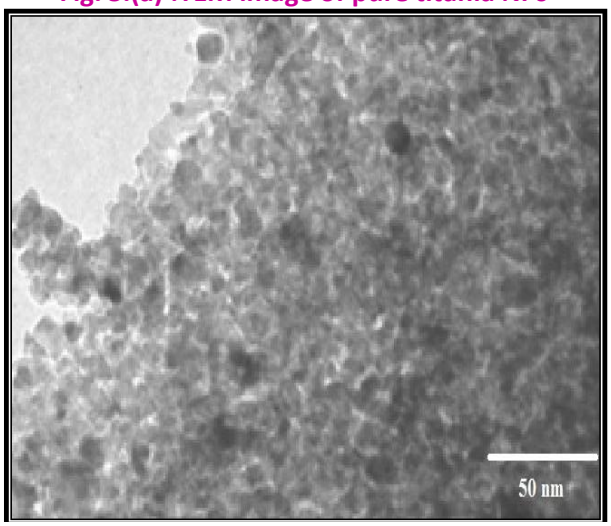

Fig. 5.(b) :TEM image of silver supported titania nanoparticles

3.4 Energy-dispersive Atomic X-ray spectroscopy (EDAX) studies

The EDAX pattern of the representative titania supported silver NPs is shown in Fig.6. Table .2 shows the compositional parameters of the elements present in the supported silver NPs. In pure titania sample, there is only peaks for titanium and oxygen without elemental silver. In other supported samples, there are

the characteristics peaks of silver, titanium and oxygen with the desired stiochiometric ratio of Ag:Ti. The obtained results are in good agreement with the theoretical compositions of the elements in all the samples.

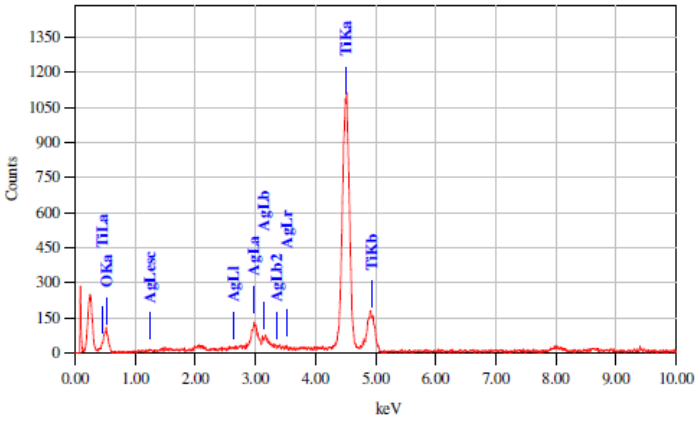

Fig. 6. EDAX pattern of silver decorated NPs titania NPs

Table: 2 Elemental composition of silver decorated NPs titania NPs

mole% Ag:TiO_2 nanoparticles	Elemental composition (atomic %)		
	Ag (L - 2. 983 KeV)	Ti (K - 4.508 KeV)	O (K - 0.525 KeV)
0.0	--	29.54	70.54
0.5	0.52	21.46	78.03
1.0	0.98	26.99	72.03
2.0	1.98	33.78	64.32

3.5 Fourier Transformed Infrared Spectroscopy (FT-IR) studies

The FI-IR spectra of sodium dodecyl sulphate (SDS) capped silver NPs and pure titania shown in the Fig.7. The absorption band of 2950–2850 cm^{-1} recognized to aliphatic group while 1216 cm^{-1} band also indicates to presence of sulfonic acid group in SDS [43]. In the titania supported silver NPs shows wide range of 3500 to 2800 cm^{-1} confirm that O-H band. While bands at 590 cm^{-1} and 645 cm^{-1} shows antase phase of titania [44].

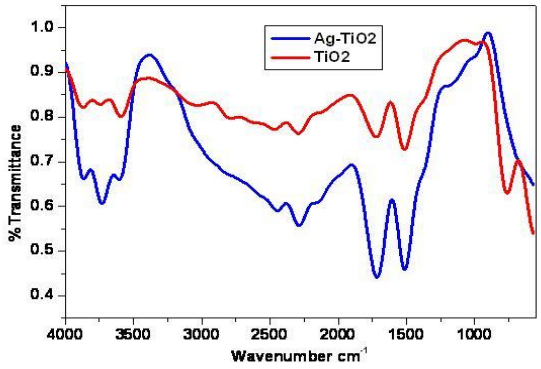

Fig. 7: FT-IR spectra of pure titania and silver NPs decorated on Titania

4 CATALYTIC STUDIES

4.1 Catalytic activity

In depth the reduction of 4-Nitrophenol (4-NP) in presence of $NaBH_4$ with titania supported silver NPs catalyst were studied. Aqueous solution of 4-NP shows characteristic absorption maximum at 317 nm due to the $n \longrightarrow \pi^*$ transition Fig. 8 [45]. In the 4-NP solution freshly prepared aqueous $NaBH_4$ solution were

added, the peak position of 4-NP red shifted to 400 nm. This designates the formation of 4-nitrophenolate ion in alkaline solution. The peak at 400 nm remained unchanged even for a couple of days in the absence of any catalyst. Addition of 0.003gm of catalyst in the reaction mixture gradually fading of characteristic of yellow due to 4-NP and finally complete bleaching of yellow due color of the 4-NP solution was observed. This reaction was complete monitored by UV-visible spectrometer with respect to time. The successive decrease peak height of 400 nm with time period was observed. In the intermediate stage of reduction no peak at 430 nm due to the Ag^0 plasmon band was observed. This may be the peak due to the Ag^0plasmon band that remained masked within the absorption band of the nitro-compounds. After all completion of reaction new peak observed at 295 nm along with disappearance of 400 nm peak confirm that reduction of 4-NP to 4-AP observed in Fig. 9. The peak observed at 295 nm is due to 4-AP because the same peakwas observed for an authentic 4-AP solution under alike experimental conditions. The various kinetic parameters for reduction of 4-NP to 4-AP is as shown in Table.3. The schematic representation of conversion of 4-nitrophenol to 4- aminophenol as given below.

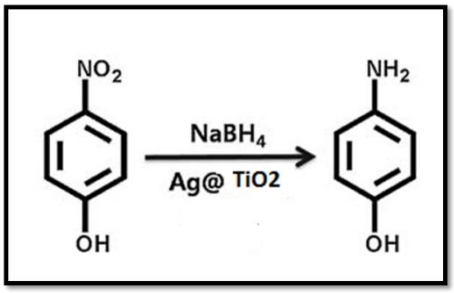

Schematic representation of conversion of 4-nitrophenol to 4- aminophenol

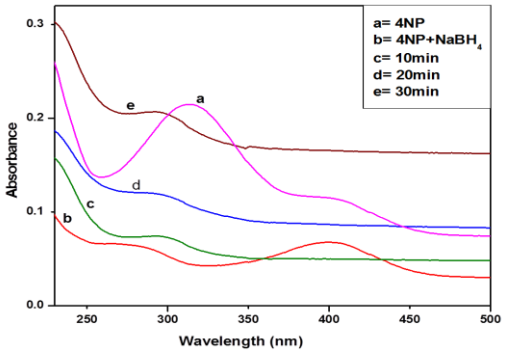

Fig. 8: UV-Visible spectra of catalytic study of reduction of 4-NP to 4-AP.

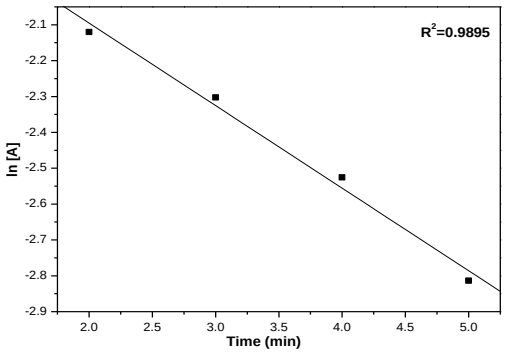

Fig. 9: Plot of ln [A] against time for the reduction of 4–NP using supported silver nanoparticles as a catalyst. Conditions: 4-NP = ($5x10^{-4}$ M) and $NaBH_4$ =(0.01M)

Table 3: Kinetic parameters for catalytic conversion of 4–nitrophenol to 4–aminophenol with respect to time

Sr.No.	Amount of supported Ag NPs	Initial Conc^{n}. of 4–NP	Conc^{n}. remained after 3 min.	Initial conc^{n}. of 4–NP	Conc^{n}. of 4–NP remained after 3min	Rate constant min^{-1}
	g	M	M	%	%	
1	0.001	0.0043	0.0001763	100	41	0.2972
2	0.003	0.0043	0.000129	100	3	1.1690
3	0.005	0.0043	0.000559	100	13	0.6801

4.2 Effect of amount of catalyst on rate of reaction

The role of metal particles is important in the catalytic reaction. So that amount of catalyst in the reaction mixture is varied while other parameter kept constant. An aqueous solution of containing 4-NP (50µl,5x10^{-4} M) and $NaBH_4$(700 µl, 0.01M) was taken in quartz cuvette. Now varying amounts of solid catalyst were added to the reaction mixture. Time- dependent reduction of 4-NP was studied spectrophotometrically by the successive decrease in the absorbance value at 400 nm and the successive increase in the absorbance value at 295 nm. With increase in amount of catalyst the rate of reaction was increased. The rate values are plotted against amount of catalyst as shown in Fig. 10.

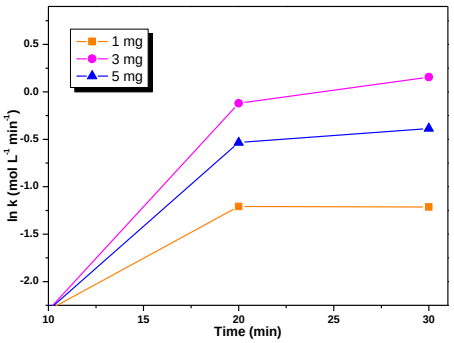

Fig. 10: Plot of ln k against time for the reduction of 4–NP using variable catalyst amount. Conditions: 4-NP = (5x10-^{4} M) and $NaBH_4$ = (0.01M)

4.3. Reusability of the catalyst

The study of reusability of catalyst was important for economical methods. During the experiment catalyst was easily recovered by centrifugation. While due to heterogeneous nature of catalyst useful for number of chemical reaction. after the first cycle, the catalyst was centrifuged, washed with water and dried at 100^{o}C for 1 h and then which was recycled for three successive cycles without significant loss of its activity. However the stability of the catalyst is more even three cycles shown in Fig. 11.

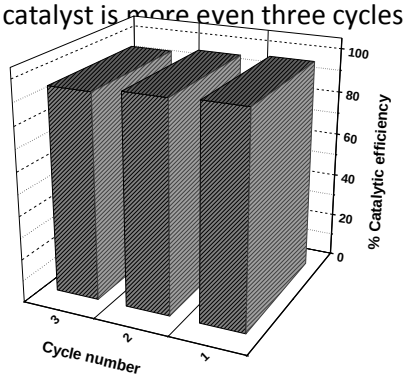

Fig. 11: Catalytic activities of Ag/TiO_2 NPs over three successive reuse cycles. Conditions: 4-NP = (5x10-^{4} M) and $NaBH_4$ = (0.01M)

5 CONCLUSION

We have successfully synthesized silver NPs by using chemical reduction method and these synthesized Ag NPs supported on the titania host lattice. XRD, TEM and EDAX revealed the formation of elemental Ag NPs rather than the silver oxides. From the TEM study, we observed the average particle size in the range of 15–20 nm with well dispersion of silver particles on titania supportive matrix. These decorated silver NPs were found to be one of the excellent catalyst towards reduction of 4-NP to 4-AP at room temperature. Therefore, it reveals that the commercial exploitation of this heterogeneous catalyst for the reduction of nitro compounds.

REFERENCES

[1] J.M. Campelo, D. Luna, R. Luque, J.M. Marinas, A.A. Romero, Chem Sus Chem, 2(2009) 18.
[2] D.P. Wang, D.B. Sun, H.Y. Yu, Z.G .Qiu, H.M. Meng, Materials Chemistry and Physics, 113 (2009) 227.
[3] H. Karamiand, E. Mohammadzadeh, International Journal of Electrochemical Science, 5 (2010) 1032.
[4] J.W. Jang, J.E. Junand, J.W. Park, Water Science and Technology, 59 (2009) 2503.
[5] S. Senapati, S.K. Srivastava, S.B.Singh, K.Biswas, Crystal Growth and Design, 10 (2010) 4068.
[6] S. Zeng , D. Baillargeat , H.P. Ho, K.T. Yong, Chemical society review, 43 (2014) 3426.452
[7] M.E. Díaz-García Analytica Chimica Acta, 666 (2010) 1.
[8] M.H. Rashid, T.K. Mandal Journal Physical Chemistry C, 111(2007)16750.
[9] Y. Zhang, S. Liu, L. Wang , X. Qin, J. Tian, W. Lu, G. Chang, X.Sun, RSC Advance**, 2 (**2012) 538.
[10] C.M. Cobley, J. Chen, E.C. Cho, L.V. Wang, Y. Xia, Chemical Society Reviews, 40 (2011) 44.
[11] B. Lim, M. Jiang, P.H.C. Camargo, E.C. Cho, J. Tao, X. Lu, Y. Zhu, Y. Xia, Science, 324 (2009) 1302.
[12] J.N. Anker, W.P. Hall, O. Lyandres, N.C. Shah, J. Zhao, R.P. VanDuyne, Nature Materials, 7 (2008) 442.
[13] T. Bala, S.K. Arumugam, R. Pasricha, B.L.V. Prasad, M. Sastry, Journal of Materials Chemistry, 14 (2004) 1057.
[14] H. Wu, X. Huang, M. Gao, X. Liao, B. Shi, Green Chemistry, 13 (2011) 651.
[15] R. Narayanan, M.A. El-Sayed, Journal of the American Chemical Society, 126 (2004) 7194.
[16] Y.S Shon, E. Cutler, Langmuir, 20 (2004) 6626.
[17] S. Tan, M. Erol, A. Attygalle, H. Du, S. Sukhishvili, Langmuir, 23 (2007) 9836.
[18] Y. Zhu, Y. Qian, X. Li, M. Zhang, Chemical Communications, 14 (1997) 1081.
[19] L.P. Jiang, S. Xu, J.M Zhu,. J.R. Zhang, J.J. Zhu, H.Y Chen, Inorganic Chemistry, 43 (2004) 5877.
[20] Y. Tan, Y. Li, D. Zhu, Journal of Colloid and Interface Science, 258 (2003) 244.
[21] D. Yu, V.W.W Yam, Journal of the American Chemical Society, 126 (2004) 13200.
[22] M. Giersig, I. Pastoriza-Santos, L.M. Liz-Marzan, Journal of Materials Chemistry, 14 (2004) 607.
[23] Y. Sun, Y. Yin, B.T. Mayers, T. Herricks, Y. Xia, Chemistry Materials, 14 (2002) 4736.
[24] B. Baruah, G.J. Gabriel, M.J. Akbashev, M.E. Booher, Langmuir, 29 (2013) 4225.
[25] H. Li, L. Han, J. Cooper-White, I. Kim, Green Chemistry, 14 (2012) 586.
[26] L. You, Y. Mao, J. Ge, Journal of Physical Chemistry C, 116 (2012) 10753.
[27] M. Choi, Z. Wu, E. Iglesia, Journal of the American Chemical Society, 132 (2010) 9129.
[28] Z.W. Seh, S. Liu, S.Y. Zhang, K.W. Shah, M.Y. Han, Chemical Communications, 47 (2011) 6689.
[29] X. Li, X. Wang, S. Song, D. Liu, H. Zhang, Chemistry–A European Journal, 18 (2012)7601.
[30] G. Vilé, D. Baudouin, I.N. Remediakis, C. Copéret, N. López, J. Pérez-Ramírez, Chem CatChem, 5 (2013) 3750.
[31] K.de O. Santos, W.C. Elias, A.M. Signori, F.C. Giacomelli, H. Yang, J.B. Domingos, The Journal Physical Chemistry C, 116 (2012) 4594.
[32] S. Laursen, S. Linic, Physical Review Letters, 97 (2006) 026101.
[33] D. Pillay, G.S. Hwang, Physical Review B, 72 (2005) 205422.
[34] E. Oakton, G. Vilé, D.S. Levine, E. Zocher, D. Baudouin, J. Pérez-Ramírez C. Copéret, Dalton Transactions, 43 (2014)15138.
[35] T. Mitsudome, Y. Mikami, H. Mori, S. Arita, T. Mizugaki, K. Jitsukawa, K. Kaned, Chemical Communication, (2009) 3258.
[36] S.D. Delekar, H.M. Yadav, S.N. Achary, S.S. Meena, S.H. Pawar, Applied Surface Science 263 (2012) 536.
[37] Y. Luo, Indian Journal of Chemistry, Section A 46 (2007) 1266.

[38] M. Gutierrez, A. Henglein, Journal Physical .Chemistry B, 97 (1993) 11368.
[39] S.P. Deshmukh, R.K. Dhokale, H.M. Yadav, S.N. Achary, S.D. Delekar, Applied Surface Science 273 (2013) 676.
[40] M. K. Seery, R. George, P. Floris, S. C. Pillai, Journal Photochemistry and Photobiology A, 189 (2007) 258.
[41] J. Virkutyte, R. S. Varma RSC Advances, 2 (2012) 2399.
[42] J. Liu, Z. Wang, Z. Luod, S. Bashir, Dalton Trans, 42 (2013) 2158.
[43] M.S. Bakshi, G. Kaur, P. Thakur, T.S. Banipal, F. Possmayer, N.O. Petersen, Journal of Physical Chemistry C 111 (2007) 5932.
[44] K. Bhattacharyya, S. Varma, A.K. Tripathi, S.R. Bharadwaj, A.K. Tyagi, Journal of Physical Chemistry C 112 (2008) 19102.
[45] S. Praharaj, S. Nath, S.K. Ghosh, S. Kundu, T. Pal, Langmuir 20 (2004) 9889.